A Lyapunov-Krasovskii Stability Analysis for Game-Theoretic Based Power Control in Optical Networks

Nem Stefanovic
University of Toronto
10 King's College Road
Toronto, Ontario, Canada
M5S 3G4
nem@control.utoronto.ca

Lacra Pavel
University of Toronto
10 King's College Road
Toronto, Ontario, Canada
M5S 3G4
pavel@control.utoronto.ca

ABSTRACT

We analyze the stability of a game-theoretic based power control algorithm for optical networks in the presence of time-delays. The control objective is to achieve optimal optical signal to noise ratio (OSNR) values for the signal channels. The control algorithms regularly adjust the signal powers entering the network based on a game-theoretic model. Each signal power is modeled as a player, whose goal is to maximize its own utility function. The utility function increases with an increasing OSNR value, and hence requires an increasing signal power. The trade-off is that if one player increases its OSNR value, this adversely affects the OSNR values of all of the other players. In addition to the signal powers, a dynamic price parameter is fed back to the power control algorithms. Time-delay is present for both the channel pricing parameter and the OSNR feedbacks in the network. We study the stability of the closed loop, time-delay system. The work utilizes singular perturbation theory modified to handle Lyapunov-Krasovskii techniques.

Keywords

Optical networks, Power control, Lyapunov-Krasovskii theory, singular-perturbation theory

1. INTRODUCTION

The core of the Internet is comprised of high-speed optical communication links. These links connect through nodes in major urban centers throughout the world to form a global optical network. Optical networks span thousands of kilometers over continents and oceans.

The primary concern in designing an optical network is to minimize transmission errors. There is a direct correlation between the optical signal to noise ratio (OSNR) in a channel and its bit-error rate. The higher the OSNR value, the lower the bit-error in a signal. A non-cooperative game between the signal powers is presented in [12]. Each channel power is modeled as a player in a game. The objective of each player is to maximize their utility function, which involves maximizing their OSNR value, and hence maximizing their signal powers. As one player increases its signal power to maximize its utility and OSNR values, the player adversely affects the other players' utility and OSNR values. The work in [12] derives a power control algorithm based on this game-theoretic approach that converges to a unique Nash equilibrium. In addition, [13] extends the work of [12] to include a channel price algorithm at the network links. This results in a primal-dual control law.

Optical networks span thousands of square kilometers, and hence, introduce significant propagation delay into their channel signals. A relatively short optical link that is $100km$ long introduces a $1ms$ round trip time-delay into a signal. A series of such links can easily introduce time-delays in the tens of milliseconds. These time delays are not accounted for in the models in [12] and [13], and as a result, their presence may destabilize the closed loop system. In essence, a convergent control algorithm for the OSNR optimization problem is not guaranteed in the presence of time-delays.

Primal-dual control laws are an active research area in communications literature. A series of papers [9, 10, 15–17] are pivotal for the work presented herein. The main body of work by Paganini et. al. is extended in [15–17] to utilize Lyapunov analysis techniques. These papers also use timescale decoupling which we also use herein. The drawbacks to these papers is in the restriction to the single-source single-link case and the decoupled utility functions with respect to the states. The paper [11] summarizes the time-delay work by Paganini et. al. A passivity approach is used in [18] that results in a generalization of several flow control schemes in literature. The control schemes in [18] show a number of similarities to those in optical networks due to gradient-like positive projection dynamics and the use of primal-dual algorithms. However, unlike in optical networks, the utility function is decoupled with respect to the state variables. A good survey paper that uses a positive projection gradient algorithm is [7]. An interesting reference for the application of Lyapunov analysis to time-delayed systems is found in [8]. The stability of ABR congestion control is studied in [1]. The work exploits time-scale decoupling using a boundary layer approach. The work studies nonlinear time-delay equations, but assumes that the slowly varying variable is fixed. In addition, [1] relies on heuristic approximations in their work. We apply a more rigorous theoretical analysis. Another paper [5] studies convergence, given time delays, for replicator dynamics applied to evolutionary sta-

Gamecomm 2008 October 20, 2008, Athens, GREECE

ble strategies in symmetric evolutionary games. The work uses linearization and frequency domain techniques to study time-delay. We can not apply a frequency domain approach to our nonlinear system herein. The work [2] considers fixed heterogeneous delays in the network using Lyapunov stability theory. To study time-delays in optical networks we rely on Lyapunov-Krasovskii stability theory as in [4]. We couple this technique with the singular-perturbation approach as in [6], but modified to handle functional equations. Finally, an interesting paper on transport delays and computing end-to-end delays in optical networks is [3]. The work motivates the study of time-delay in optical networks by studying the inefficiencies of deflection routing. Their analysis is based on Markov chains. We use deterministic models herein. Optical networks are multi-input multi-output systems characterized by a coupled utility function, and with decentralized control laws.

In this paper, we analyze the stability of optical power control algorithms based on [12] and [13] in the presence of time-delays. Specifically, we study the modified model of [14] where the channel price algorithm is moved from the links to the sources. Unlike [14] which analyzes the closed loop system using Lyapunov-Razumikhin techniques, we present an alternative approach that uses the more general Lyapunov-Krasovskii theory. We also use singular perturbation theory modified to handle the functional Lyapunov equations needed for Lyapunov-Krasovskii theory. We obtain sufficient results to ensure the stability of the time-delayed system given that the delay satisfies an upper bound. A tunable gain at the sources is our design variable.

The paper is organized as follows. Section 2 reviews the OSNR model, control algorithms and link algorithms. Section 3 reviews the closed-loop time-delay system derived in [14]. Section 4 presents the main stability result and corresponding proof. A scalar analysis is performed in section 5 and the results are contrasted with [14]. Section 6 provides simulation results with comparison to the Lyapunov-Razumikhin simulations from [14]. The last section provides conclusions and future work. The appendix provides the lemma proofs.

2. REVIEW OF OSNR MODEL AND CONTROL ALGORITHMS

We begin by reviewing the OSNR model. The discrete-time control algorithm from [12] is presented next. We then introduce the link control law from [13].

2.1 OSNR Model

Consider an optical network that is defined by a single optical link. Channels in the network can be added or dropped. The link is composed of N spans that include one optical amplifier per span. A set of channels, $M = \{1, ..., m\}$, (intensity modulated wavelengths) are multiplexed together and transmitted across the link. We denote u_i, s_i, and n_i, the optical input power for channel i at the transmitter (Tx), the output signal at the receiver (Rx), and the output noise at Rx, respectively. The Optical Signal-to-Noise Ratio (OSNR) for any channel, $i \in M$, is defined as

$$OSNR_i = \frac{s_i}{n_i} \tag{1}$$

The following provides the framework for modeling OSNR in a single link optical network. An optical span is composed of an optical amplifier (OA) with channel dependent gain, G_i and optical fiber with wavelength independent loss coefficient, L_k. The amplifiers have the same spectral shape and are operated in automatic power control (APC) mode with total power targets P_0. The OA introduces amplified spontaneous emission (ASE) noise power, denoted $ASE_{k,i}$.

The following lemma from [12] describes the OSNR model for an optical link.

Lemma 1. *The OSNR for the i^{th} channel is given as*

$$OSNR_i = \frac{u_i}{n_{0,i} + \sum_{j \in M} \Gamma_{i,j} u_j} \tag{2}$$

where $\Gamma_{i,j}$, elements of the full $(n \times n)$ system matrix Γ, are defined as

$$\Gamma_{i,j} = \sum_{k=1}^{N} \frac{G_j^k}{G_i^k} \frac{ASE_{k,i}}{P_0}$$

and $n_{0,i}$ is the noise optical power at transmitter (Tx) for the i^{th} channel.

With Lemma 1 presented, we can next introduce the primal-dual control law presented in [13]. The control law is introduced in two parts, the channel algorithm and the link algorithm. The channel algorithm is the same game-theoretic algorithm derived in [12] with the exception that the constant cost parameter, α_i is substituted for an adjustable variable $\mu(\bar{k})$. The link algorithm is a computed every K iterations of the channel algorithm at the network links. Its purpose is to feedback the channel price parameter $\mu(\bar{k})$ to the channel sources.

2.2 Channel Algorithm

Given the OSNR model in Lemma 1, a non-cooperative game between channels was defined in [12]. The objective of each channel (player) is to maximize its utility related to OSNR in the presence of other channels. We use the utility function [12]

$$U_i = ln\left(1 + a_i \frac{OSNR_i}{1 - \Gamma_{i,i} OSNR_i}\right)$$

where a_i is a channel dependent design parameter. A greater utility implies greater OSNR values which further implies a lower bit error rate in the optical network. Each channel adjusts its power towards this goal in the presence of other channels. The game settles at an equilibrium when no channel can improve its utility unilaterally; the equilibrium of the game being a Nash equilibrium. By converging to the Nash equilibrium the distributed system will achieve optimal OSNR values for its channels without centralized control. A full Nash game solution was presented in [12]. This work was then modified in [13] to include an adjustable cost parameter, μ, that reflects the network channel utilization. The OSNR game admits a unique Nash equilibrium, u^*, which is the solution of

$$a_i u_i^* + \sum_{j \neq i} \Gamma_{i,j} u_j^* = \frac{a_i \beta_i}{\mu(\bar{k})} - n_{0,i} \quad \forall i \tag{3}$$

Based on this solution an iterative network level control algorithm was proposed in [12] to control the system (2) at the sources

$$u_i(k+1) = \frac{\beta_i}{\mu(\bar{k})} - \frac{1}{a_i}\left(\frac{1}{OSNR_i(k)} - \Gamma_{i,i}\right) u_i(k) \tag{4}$$

where β_i and a_i are design parameters and k is the iteration time step. The parameter $\mu(\bar{k})$ is the channel price. The control algorithm (4) converges to the Nash equilibrium (3) if

$$a_i > \sum_{j \neq i} \Gamma_{i,j} \tag{5}$$

2.3 Link Algorithm

The link algorithm is computed every K iterations of the control algorithm (4). The value K is a large number such that the link algorithm is updated infrequently with respect to the control algorithm (ie. K=100). The link algorithm [13] is:

$$\mu(\bar{k}+1) = [\mu(\bar{k}) + \eta(\sum_{j=1} u_j(K) - P_0)]^+$$

where η is the step-size and $[z]^+ = max\{z, 0\}$. The variable $\bar{k}$ represents the discrete-time variable which is on a different time-scale than the control algorithm (4). Under normal operations, $\mu(\bar{k})$ must be greater than zero because it enters (4) inverted. Thus, similarly to [7], we drop $[\cdot]^+$ in the ensuing analysis to obtain

$$\mu(\bar{k}+1) = \mu(\bar{k}) + \eta(\sum_{j=1} u_j(K) - P_0) \tag{6}$$

Notice that $\sum_{j=1} u_j(K)$ is the received total power for all channels in the link. This is easily measured in practice as a real-time value. Moreover, under the assumption of stationary channel powers, which can be made given that the link algorithm updates very slowly, the link algorithm corresponds to a gradient descent technique. The combined channel-link algorithm converges to the optimal NE channel power and price (u^*, μ^*) [13].

Figure 1 depicts the control algorithm (4) and the link algorithm (6) acting on the OSNR system (2). Despite having a convergent control algorithm for the OSNR optimization problem, the practical implementation of such a control law has to take time-delay into account.

3. CONTINUOUS-TIME CLOSED LOOP SYSTEM WITH TIME-DELAY

In this section, we outline the derivation of the closed loop continuous-time system with time-delay as in [14]. We first review the time-delay version of the OSNR model (2). The control gains ρ_i, $0 < \rho_i \leq 1$, for each channel i, are included as control parameters at the sources. We interconnect the control algorithm (4) with the link algorithm (6) together at the sources. The closed loop system including time-delays is presented in continuous-time form.

The OSNR model (2) does not take time-delay into account. Forward time-delay occurs from the channel sources u_j to the OSNR outputs $OSNR_i$ at the end of the link. We adopt the notation that $\tau_f \geq 0$ represents the forward time-delay. Similarly, the backward time-delay occurs from the OSNR outputs $OSNR_i$ back to its associated source u_i. We denote this time-delay as τ_b. We denote $\tau = \tau_f + \tau_b$ as the total round trip delay. We modify (2), (10) and (9) to include time-delay.

We explicitly introduce forward time-delay into (2) as

$$OSNR_i(t) = \frac{u_i(t-\tau_f)}{n_{0,i} + \Sigma_{j \in M} \Gamma_{i,j} u_j(t-\tau_f)} \tag{7}$$

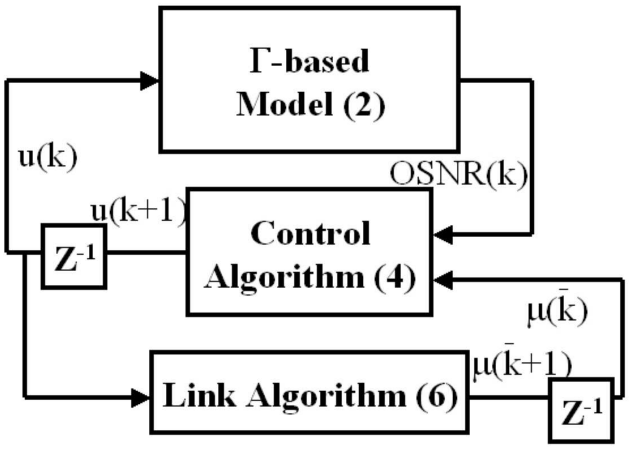

Figure 1: Discrete-time Control Algorithm (4) and Link Algorithm (6) applied to OSNR system (2)

so that $OSNR_i(t)$ depends on delayed input signals.

The algorithm (10) applied at the sources (Tx) will use a delayed version of (7) due to the backward time-delay, i.e. $OSNR_i(t-\tau_b)$. Denote the round-trip time-delayed OSNR model as

$$OSNR_i(t) = \frac{u_i(t-\tau)}{n_{0,i} + \Sigma_{j \in M} \Gamma_{i,j} u_j(t-\tau)} \tag{8}$$

From [14], the continuous-time versions of (4) and (6) with tuning parameters ρ_i is

$$\dot{\mu(t)} = \eta(\sum_{j=1} u_j(t) - P_0) \tag{9}$$

$$\frac{du_i(t)}{dt_f} = \rho_i \left\{ \frac{\beta_i}{\mu(\bar{k})} - \frac{1}{a_i} \left(\frac{1}{OSNR_i(t)} - \Gamma_{i,i} + a_i \right) u_i(t) \right\} \tag{10}$$

where t_f denotes the "fast" time variable. We can relate the link algorithm time variable, t, to t_f according to the relation $t_f = tK$. Let $\epsilon = \frac{1}{K}$, then

$$\frac{du_i}{dt_f} = \frac{du_i}{dt}\frac{dt}{dt_f} = \epsilon \frac{du_i}{dt} \tag{11}$$

Substituting (8) into (10), and using (11), gives

$$\epsilon \frac{du_i(t)}{dt} = \rho_i \left\{ \frac{\beta_i}{\mu(t)} - \frac{1}{a_i} \left(\frac{n_{0,i} + \sum_j \Gamma_{i,j} u_j(t-\tau)}{u_i(t-\tau)} - \Gamma_{i,i} + a_i \right) u_i(t) \right\} \tag{12}$$

Since (12) derives from our control algorithm, we can modify (12) to eliminate $u_i(t-\tau)$ in the denominator by design. Notice that if we keep a record of past power inputs, $u_i(t-\tau)$, we can then appropriately replace $u_i(t)$ with $u_i(t-\tau)$ to obtain

$$\epsilon \frac{du_i(t)}{dt} = \rho_i \left\{ \frac{\beta_i}{\mu(t)} - \frac{1}{a_i} \left(n_{0,i} + \sum_j \Gamma_{i,j} u_j(t-\tau) \right) + \left(\frac{\Gamma_{i,i}}{a_i} - 1 \right) u_i(t) \right\} \tag{13}$$

Thus, (13) and (9) represent the closed loop system with time-delay. This closed loop system representation has both

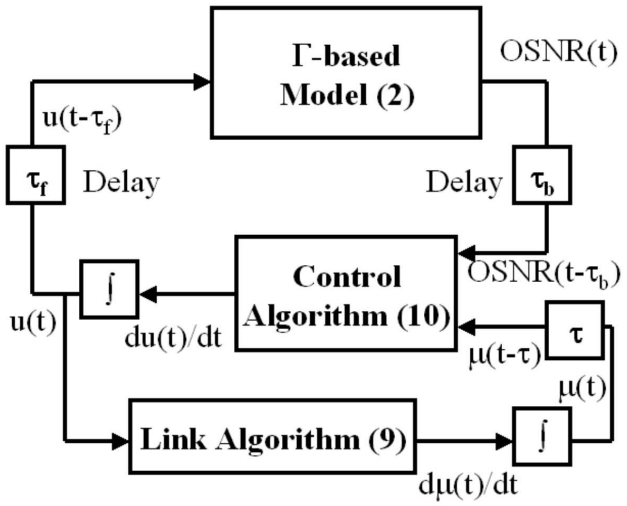

Figure 2: Continuous-time Control Algorithm (10) and Link Algorithm (9) at the sources

the channel control algorithms (10) and the channel price algorithm (9).

When the time-delay, τ, in (13) and (9) is set equal to zero, the equilibrium point of the system becomes (3) and

$$\sum_j u_j^* = P_0 \tag{14}$$

If we shift (13) and (9) around the equilibrium point (14) and (3) we get the resultant closed loop, time-delayed system

$$\dot{x}(t) = \eta(\textstyle\sum_{j=1} z_j(t)) \tag{15}$$

$$\epsilon \tfrac{dz_i(t)}{dt} = \rho_i \left\{ \tfrac{\beta_i}{x(t-\tau)+\mu^*} - \tfrac{\beta_i}{\mu^*} - \tfrac{1}{a_i} \textstyle\sum_j \tilde{\Gamma}_{i,j} z_j(t-\tau) \right\} \tag{16}$$

where we have artificially introduced a time delay of τ in the x variable of (16) to simplify the foregoing analysis. We also define $\tilde{\Gamma}_{i,j}$ as

$$\tilde{\Gamma}_{i,j} = \begin{cases} a_i, & i = j \\ \Gamma_{i,j}, & i \neq j \end{cases} \tag{17}$$

4. MAIN RESULT

We apply singular perturbation theory modified to work with Lyapunov-Krasovskii techniques to analyze the stability of the closed loop, time-delay system (15) and (16). Our approach yields sufficient conditions for stability.

To use functional equations, we first define $\mathcal{C}([-r,0],\Re^n)$ as the set of all continuous functions mapping $[-r,0]$ to $\Re^n$. We simplify the notation by letting $\mathcal{C} = \mathcal{C}([-r,0],\Re^n)$. The following definition will be used with Lyapunov-Krasovskii theory and the proof of the main theorem herein.

***Definition** 1.* The continuous norm is defined as

$$||y_t||_c = max_{-r \leq \theta \leq 0} ||y(t+\theta)||_2$$

where $y_t \in \mathcal{C}$, represents the set of values, $y(q)$, for all $q \in [t-r,t]$.

Note that $||y(t)||_2 \leq ||y_t||_c$. We use the following definition of stability from [4],

***Definition** 2.* Consider the general system

$$\dot{\bar{x}} = F(t, \bar{x}_t) \tag{18}$$

where $\bar{x}_t \in \mathcal{C}$ represents the set of values $\bar{x}(q)$ for all $q \in [t-r,t]$ and $F : \Re \times \mathcal{C} \rightarrow \Re^n$. We say (18) is stable if for any $t_0 \in \Re$ and any $\epsilon > 0$, there exists a $\delta = \delta(t_0, \epsilon) > 0$ such that $||\bar{x}_{t_0}||_c < \delta$ implies $||\bar{x}(t)||_2 < \epsilon$ for $t \geq t_0$. System (18) is asymptotically stable if it is stable and $lim_{t\rightarrow\infty} \bar{x}(t) = 0$.

We state the restricted Lyapunov-Krasovskii theorem [4](Proposition 5.2, pg.150) that gives general conditions for asymptotic stability for time-delay systems based on Definition 2.

Theorem 1. *A time-delay system is asymptotically stable if there exists a Lyapunov-Krasovskii functional V such that for some $\psi > 0$ and $K > 0$, it satisfies*

$$\psi ||y(t)||_2^2 \leq V(y_t) \leq K ||y_t||_c^2$$

where the continuous norm $||y_t||_c$ is defined in Definition 1. The derivative of $V(y_t)$ along the system trajectory $\dot{V}(y_t)$ satisfies

$$\dot{V}(y_t) \leq -\psi ||y(t)||_2^2$$

Theorem 1 is more general than Lyapunov-Razumikhin theory [4].

Next, we re-write (15) and (16) in the form

$$\dot{x} = f(z) \tag{19}$$

$$\epsilon \dot{z} = g(x(t-\tau), z(t-\tau)) \tag{20}$$

We now define the reduced and boundary-layer systems.

***Definition** 3.* Consider the system (19) and (20). Let the reduced system be defined as

$$\dot{x} = f(h(x))$$

and the boundary system be defined as

$$\frac{dy}{dt_f} = g(x(t-\tau), y(t-\tau) + h(x(t-\tau)))$$

where $h(x)$ is the isolated root from the RHS of (20), t_f is defined as in (11), and $y = z - h(x)$ is a co-ordinate shift.

Apply Definition 3 to (15) and (16)

$$\dot{x} = \eta 1_{row} \tilde{\Gamma}_a^{-1} \beta \left(\tfrac{1}{x+\mu^*} - \tfrac{1}{\mu^*} \right) \tag{21}$$

$$\tfrac{dy}{dt_f} = -\rho \tilde{\Gamma}_a y(t-\tau) \tag{22}$$

where 1_{row} is a row vector of 1 elements, and

$$h(x) = \tilde{\Gamma}_a^{-1} \beta \left(\frac{1}{x(t)+\mu^*} - \frac{1}{\mu^*} \right) \tag{23}$$

where (21) is the reduced system and (22) is the boundary layer system. The reduced system (21) is nonlinear and scalar with no time-delay. The boundary layer system (22) is a linear system, with one constant time-delay. The reduced and boundary layer forms of (15) and (16) simplify the nonlinear analysis.

The following lemmas are used to prove the main theorem. Their proofs can be found in appendix A.

Lemma 2. *The boundary-layer system (22) is exponentially stable if*

$$\tau < \frac{x^2 s - c_3 s - 2\bar{y}c_3}{2xc_3} - \frac{\sqrt{(x^2 s - c_3 s - 2\bar{y}c_3)^2 + 4c_3 x^2(s^2 + 2\bar{y}s + c_1)}}{2xc_3} \quad (24)$$

where

$$c_1 = \bar{\sigma}\left((A_1^T P - \bar{y}I)(PA_1 - \bar{y}I)\right) \quad (25)$$

$$c_3 = \bar{y}^2\bar{\sigma}(A_1^T A_1) \quad (26)$$

and $P > 0$, and $A_1 = -\rho\tilde{\Gamma}_a$. The variables $x > 0$, $-\bar{y} - \sqrt{\bar{y}^2 - c_1} < s < -\bar{y} + \sqrt{\bar{y}^2 - c_1}$ and $\bar{y} < -\sqrt{c_1}$, are design variables. The matrix $\tilde{\Gamma}_a$ has elements $\tilde{\Gamma}_{i,j}/a_i$ with $\tilde{\Gamma}_{i,j}$ in (17). In addition, $\rho = diag(\rho_i)$ and $\bar{\sigma}(\cdot)$,$\underline{\sigma}(\cdot)$ denote the largest and smallest singular value [19].

Given the A_1 matrix, equation (24) can be made optimal numerically, i.e., picking optimal x, y, and s parameters to maximize the upper bound, using constrained optimization.

Lemma 3. *The reduced system (21) is exponentially stable if*

$$a_i > \frac{1}{2}\sum_{j\neq i}(\Gamma_{i,j} + \Gamma_{j,i}) \quad (27)$$

Theorem 2. *For the singularly perturbed system (15) and (16), there exists $\epsilon^* > 0$ such that for $0 < \epsilon < \epsilon^*$, and for η sufficiently small, the origin is asymptotically stable if (24) and (27) are satisfied.*

Proof We use the singular perturbation approach [6], but modified to handle time-delays as needed for (15) and (16). Note that $f(0) = 0$, $g(0, 0) = 0$, and $h(0) = 0$.

We apply a similar approach to [14], but with a functional Lyapunov equation. The fundamental approach of singular perturbation theory is to prove the origin of (15) and (16) is asymptotically stable using the much simpler reduced (21) and boundary-layer (22) systems. Lemmas 3 and 2 ensure exponential stability for both the reduced (21) and boundary layer (22) systems. A composite, functional Lyapunov equation is constructed from the reduced and boundary layer systems.

PART 1: REDUCED SYSTEM

The reduced system (21) is exponentially stable and does not have time-delay. We select the Lyapunov function $V(x) = \frac{1}{2}x^2$. The following properties hold,

$$V(x) = \tfrac{1}{2}||x||_2^2 \quad (28)$$

$$\tfrac{\partial V}{\partial x} f(h(x)) \leq -\tfrac{\eta 1_{row}\tilde{\Gamma}_a^{-1}\beta}{\mu^*(\mu^*+r)}||x||_2^2 \leq -k_*||x||_2^2 \quad (29)$$

$$\left|\tfrac{\partial V}{\partial x}\right| = |x| \quad (30)$$

for $x \leq r$, where $r > -\mu^*$, and $k_* > 0$ is a constant. We later show that $x \in [-r, r]$ and $r \in (-\mu^*, \mu^*)$ are the full regions for validity.

PART 2: BOUNDARY-LAYER SYSTEM

The boundary-layer system (22) is an exponentially stable, linear, time-delay system. To handle the time-delay in the stability analysis, we use Lyapunov-Krasovskii theory that is based on functional Lyapunov equations.

We pick the Lyapunov functional from [4],

$$W(y_t) = y^T(t)Py(t) + \int_{-\tau}^{0}\int_{t-\tau+\theta}^{t} y^T(\xi)\tilde{\Gamma}_a^T\rho Z\rho\tilde{\Gamma}_a y(\xi)d\xi d\theta + \int_{t-\tau}^{t} y^T(\theta)Sy(\theta)d\theta \quad (31)$$

where $P > 0$, $S > 0$, $y_t \in \mathcal{C}$, represents the set of values, $y(q)$, for all $q \in [t - \tau, t]$, and

$$\begin{pmatrix} X & Y \\ Y^T & Z \end{pmatrix} > 0 \quad (32)$$

such that $X = X^T$ and $Z = Z^T$. Note that X, Y, and Z are design variables.

Using (31), we prove time-delay stability for the boundary-layer system (22), if (24) is satisfied in Lemma 2. In fact, (22) is exponentially stable and $W(y_t)$ satisfies the following set of conditions

$$\psi||y(t)||_2^2 \leq W(y_t) \leq K||y_t||_c^2 \quad (33)$$

$$\tfrac{dW(y_t)}{dt} \leq -k||y||_2^2 \quad (34)$$

$$\left|\left|\tfrac{dW_{quad}}{dy}\right|\right|_2 = ||2y^T P||_2 \leq 2||P||_F||y||_2 \quad (35)$$

where $W_{quad} = y^T Py$, $\psi > 0$, $K > 0$ and k sufficiently small [4]. The symbol $||\cdot||_F$ is the Frobenius norm. Note that (34) is satisfied for the boundary-layer system (22) since Lemma 2 is derived using Theorem 1.

PART 3: SHIFT OF CO-ORDINATES

We rewrite (15) in matrix form,

$$\dot{x}(t) = \eta 1_{row} z(t)$$

and substitute the co-ordinate shift $y = z - h(x)$, where $h(x)$ is defined in (23),

$$\dot{x}(t) = \eta 1_{row}\left(y(t) + \tilde{\Gamma}_a^{-1}\beta\left(\frac{1}{x(t)+\mu^*} - \frac{1}{\mu^*}\right)\right) \quad (36)$$

Similarly, from (16) we obtain

$$\epsilon\dot{y} = -\rho\tilde{\Gamma}_a y(t-\tau) + \epsilon\tilde{\Gamma}_a^{-1}\beta\tfrac{\eta}{(x(t)+\mu^*)^2} \cdot 1_{row}\left(y(t) + \tilde{\Gamma}_a^{-1}\beta\left(\tfrac{1}{x(t)+\mu^*} - \tfrac{1}{\mu^*}\right)\right) \quad (37)$$

Note that the following relations are satisfied

$$||f(y + h(x)) - f(h(x))||_2 = ||\eta 1_{row} y||_2 \leq \eta\sqrt{m}||y||_2 \quad (38)$$

$$||f(h(x))||_2 \leq \tfrac{\eta 1_{row}\tilde{\Gamma}_a^{-1}\beta}{\mu^*(\mu^*-r)}||x||_2 \quad (39)$$

$$||\tfrac{\partial h(x)}{\partial x}||_2 = ||-\tilde{\Gamma}_a^{-1}\beta\tfrac{1}{(x+\mu^*)^2}||_2 \leq ||\tilde{\Gamma}_a^{-1}\beta||_2\tfrac{1}{(\mu^*-r)^2} \leq k_2 \quad (40)$$

$$||h(x)||_2 \leq ||\tilde{\Gamma}_a^{-1}\beta||_2\tfrac{||x||_2}{\mu^*(\mu^*-r)} \leq k_3||x||_2 \quad (41)$$

for $x \in [-r, r]$, where $r \in (-\mu^*, \mu^*)$, and $k_2 > 0$ and $k_3 > 0$ are constants. By (27), $1_{row}\tilde{\Gamma}_a^{-1}\beta > 0$. The constant m is the size of y.

PART 4: COMPOSITE LYAPUNOV FUNCTION

We can then define the composite Lyapunov function as $\chi(x, y_t) = V(x) + W(y_t)$, where $V(x)$ is (28), $W(y_t) = W_{quad}(y) + W_{int}(y_t)$ in (31), $W_{quad}(y) = y^T(t)Py(t)$ and $W_{int}(y_t)$ is the integral terms of (31). By applying the composite Lyapunov function, $\chi(x, y_t)$, to (37) and (36), and exploiting the Lyapunov inequalities in (28)-(35) and Lipschitz properties (38)-(41), we prove asymptotic stability by Theorem 1. The rest of the proof follows as in Theorem 11.4 [6]. We take the time-derivative of $\chi(x, y_t)$ along the

trajectory of the system (19) and (20). We also use the general functions f,g and h, where h is defined in (23), along with the co-ordinate shift $z = y + h(x)$, to obtain

$$\dot{\chi} = \frac{dW_{quad}(y)}{dy}\left[\frac{1}{\epsilon}g(x(t-\tau), y(t-\tau) + h(x(t-\tau))) - \frac{dh}{dx}f(y+h(x))\right] + \frac{d}{dt}\left[W_{int}(y_t)\right] + \frac{dV(x)}{dx}f(x, y+h(x)) \tag{42}$$

where if we substitute $W_{quad} = y^T(t)Py(t)$ and $V(x) = 1/2x^2$, we get

$$\begin{aligned}\dot{\chi} &= 2y^T(t)P\left[\frac{1}{\epsilon}g(x(t-\tau), y(t-\tau) + h(x(t-\tau))) \right.\\ &- \left. \frac{dh}{dx}f(y+h(x))\right] + \frac{d}{dt}\left[W_{int}(y_t)\right] + xf(x, y+h(x))\end{aligned} \tag{43}$$

Notice that the form of (43) is very similar in form to the form in [14], with the exception of the integral terms from $W(y_t)$ in (31). Denote by $g = g(x(t-\tau), y(t-\tau) + h(x(t-\tau)))$. From (34), the boundary layer system (22) satisfies

$$2y^T Pg + \frac{d}{dt}\left[W_{int}(y_t)\right] \leq -k||y||_2^2 \tag{44}$$

From (43), we have a slightly different form than the LHS of (44), where we satisfy

$$\frac{1}{\epsilon}2y^T Pg + \frac{d}{dt}\left[W_{int}(y_t)\right] \leq -k||y||_2^2 \tag{45}$$

if we choose $P = \epsilon\bar{P}$.

We next attain bounds on the remaining terms of (42), or equivalently (43), using the norm inequalities (28)-(35), and (38)-(40). For the last term of (43),

$$\begin{aligned}\frac{\partial V}{\partial x}f(x, y+h(x)) &= \frac{\partial V}{\partial x}[f(x, y+h(x)) - f(x, h(x))]\\ &+ \frac{\partial V}{\partial x}f(x, h(x))\end{aligned}$$

we apply (38), (39) and (30) to get

$$\begin{aligned}\frac{dV}{dx}f(x, y+h(x)) &\leq ||x||_2\eta\sqrt{m}||y||_2 - \frac{\eta 1_{row}\tilde{\Gamma}_a^{-1}\beta}{\mu^*(\mu^* - r)}||x||_2^2\\ &= L_3||x||_2||y||_2 - b_3||x||_2^2\end{aligned} \tag{46}$$

where L_3 and b_3 are constants. Finally, the only remaining term of (43) that is left is

$$\begin{aligned}\frac{dW_{quad}}{dy}\frac{dh}{dx}f(x, y+h(x)) &= \frac{dW_{quad}}{dy}\frac{dh}{dx}f(x, h(x))\\ &+ \frac{dW_{quad}}{dy}\frac{dh}{dx}[f(x, y+h(x)) - f(x, h(x))]\end{aligned}$$

we apply (35), (38), (39) and (40) to get

$$\begin{aligned}&\frac{dW_{quad}}{dy}\frac{dh}{dx}f(x, y+h(x))\\ &\leq 2\epsilon||\bar{P}||_F||y||_2||\tilde{\Gamma}_a^{-1}\beta||_2\frac{1}{(\mu^* - r)^2}\eta\sqrt{m}||y||_2\\ &+ 2\epsilon||\bar{P}||_F||y||_2||\tilde{\Gamma}_a^{-1}\beta||_2\frac{1}{(\mu^* - r)^2}\frac{\eta 1_{row}\tilde{\Gamma}_a^{-1}\beta}{\mu^*(\mu^* - r)}||x||_2\\ &= b_4\epsilon||y||_2^2 + L_4\epsilon||x||_2||y||_2\end{aligned} \tag{47}$$

where b_4 and L_4 are constants. By substituting (46) and (47) back into (43), we get

$$\begin{aligned}\dot{\chi} &\leq L_3||x||_2||y||_2 - b_3||x||_2^2 - k||y||_2^2 + \epsilon b_4||y||_2^2\\ &+ \epsilon L_4||x||_2||y||_2\end{aligned}$$

or,

$$\dot{\chi} \leq -a_1||x||_2^2 - a_3||y||_2^2 + a_5||x||_2||y||_2$$

where $a_1 = b_3$, $a_3 = k - \epsilon b_4$, and $a_5 = L_3 + \epsilon L_4$.

We can then write

$$\dot{\chi} \leq -\begin{bmatrix} ||x||_2 \\ ||y||_2 \end{bmatrix}^T \begin{bmatrix} a_1 & -\frac{a_5}{2} \\ -\frac{a_5}{2} & a_3 \end{bmatrix} \begin{bmatrix} ||x||_2 \\ ||y||_2 \end{bmatrix} \tag{48}$$

To ensure that the RHS of (48) is negative, we must ensure that $a_3 > 0$ and $a_1a_3 - a_5^2/4 > 0$. This is achieved for ϵ and η small enough. Thus, the RHS of (48) is negative. Thus, the second condition of Theorem 1 is satisfied.

Furthermore, by the Lyapunov properties, we have $\chi(x, y) = V(x) + W(y_t) \leq 1/2||x||_2^2 + K||y||_c^2$ by (28) and (33), or

$$\begin{aligned}\chi(x, y) &\leq \begin{bmatrix} ||x||_2 \\ ||y||_c \end{bmatrix}^T \begin{bmatrix} 1/2 & 0 \\ 0 & K \end{bmatrix} \begin{bmatrix} ||x||_2 \\ ||y||_c \end{bmatrix}\\ &\leq \begin{bmatrix} ||x||_c \\ ||y||_c \end{bmatrix}^T \begin{bmatrix} 1/2 & 0 \\ 0 & K \end{bmatrix} \begin{bmatrix} ||x||_c \\ ||y||_c \end{bmatrix}\end{aligned}$$

and $\chi(x, y) = V(x) + W(y_t) \geq 1/2||x||_2^2 + \psi||y||_2^2$, or

$$\chi(x, y) \geq \begin{bmatrix} ||x||_2 \\ ||y||_2 \end{bmatrix}^T \begin{bmatrix} 1/2 & 0 \\ 0 & \psi \end{bmatrix} \begin{bmatrix} ||x||_2 \\ ||y||_2 \end{bmatrix}$$

Thus, the first condition of Theorem 1 is satisfied. Hence, by Theorem 1, the closed loop system (37) and (36) is asymptotically stable. *End of Proof*

5. SCALAR ANALYSIS

In [14], the Lyapunov-Razumikhin based main theorem yields an upped bound on the time-delay τ to ensure closed loop stability for (15) and (16). This general theorem was studied in its scalar case, i.e. single link, single channel, for comparison and discussion purposes. The scalar bound was found to be $\tau < 1/(\rho\tilde{\Gamma}_a)$, where $\rho\tilde{\Gamma}_a$ is a constant. The bound (24) simplifies in the scalar case and allows itself to be directly compared to the Lyapunov-Razumikhin bound from [14]. We analyze and compare the scalar case for (24) in this section.

We use a number of results from the proof of Lemma 2 found in appendix A. From (24), in the scalar case, i.e., $\rho\tilde{\Gamma}_a$ is a constant, we get the time-bound, denoted by τ_1

$$\tau_1 = \frac{j_1 - \sqrt{j_1^2 + j_2}}{2\bar{y}^2a^2x} \tag{49}$$

where $a = -\rho\tilde{\Gamma}_a$ and

$$j_1 = x^2s - \bar{y}^2a^2s - 2\bar{y}^3a^2 \tag{50}$$

$$j_2 = 4\bar{y}^2a^2x^2(s^2 + 2\bar{y}s + (pa - \bar{y})^2) \tag{51}$$

Note that $j_1 > 0$ (see appendix A) and by (70) we have $j_2 < 0$. Equation (49) is in the same form as (66) but simplified due to the scalar case. Since $j_2 < 0$, by (71), we get the condition

$$s^2 + 2\bar{y}s + (pa - \bar{y})^2 < 0 \tag{52}$$

For (52) to hold, the LHS of (52) must have real roots, or equivalently, $p < 2\bar{y}/a$.

Note that increasing or decreasing j_1 has no effect in increasing (49), because the j_1^2 under the square root will subtract from the first j_1 term in the numerator. Thus, to optimize (49), we must minimize j_2. To minimize j_2, (51), we first select $s = -\bar{y}$ because this minimizes the terms $s^2 + 2\bar{y}s$. Then, (49) becomes

$$\tau_1 = \frac{-(\bar{y}^3a^2 + x^2\bar{y}) - \sqrt{(\bar{y}^3a^2 - x^2\bar{y})^2 + 4\bar{y}^2a^2x^2(pa - \bar{y})^2}}{2\bar{y}^2a^2x^2} \tag{53}$$

Next, we set $\bar{y} = ap$. This further minimizes j_2 and we also see it eliminates the second term under the square root in (53). Notice that the first term under the square root can be eliminated by selecting $x = ay = a^2p$. This also increases the first term in the numerator. Thus, we get,

$$\tau_1 = \frac{-2a^5p^3}{2a^6p^3} = \frac{-1}{a} = \frac{1}{\rho\tilde{\Gamma}_a} \tag{54}$$

which is exactly the same time-delay bound as in the Lyapunov-Razumikhin case from [14]. Although we used the far more general Lyapunov-Krasovskii theory, we ultimately did not increase the time-delay bound for the scalar case. Despite this, the general equation (24) is quite different in form from the time-delay bound in [14] and may yield advantages in the multi-input multi-output case. The foregoing simulations illustrate the improvements in the time-delay bounds. Also, we verified the results of [14] by an alternative approach.

We can compute the theoretical maximum time-delay bound for the scalar version of the boundary layer system (22). From [4], we can treat the representation of the characteristic quasipolynomial of (22) as a bivariate polynomial. The characteristic polynomial, $\zeta(s, e^{-\tau s})$, of (22) is:

$$\zeta(s, e^{-\tau s}) = s + \tilde{\Gamma}_a e^{-\tau s} \tag{55}$$

Then, we define $z = e^{-\tau s}$, and $\bar{\zeta} = z\zeta(-s, z^{-1})$, and represent $\zeta(s, z) = 0$ and $\bar{\zeta}(s, z) = 0$ to obtain

$$s + \rho\tilde{\Gamma}_a z = 0 \tag{56}$$

$$z(-s + \rho\tilde{\Gamma}_a z^{-1}) = 0 \tag{57}$$

Solving (56) and (57) for the maximum τ bound τ_{max} yields

$$\tau < \tau_{max} = \frac{\pi/2}{\rho\tilde{\Gamma}_a} \tag{58}$$

Thus, (58) shows that we still have the potential to improve the τ bound (54) by approximately 57 percent.

6. SIMULATIONS

In this section, we test the validity of Theorem 2 via simulations based on realistic network parameters. Table 1 lists the network parameters that were selected for the forgoing simulations.

The following design parameters are selected. We pick $a_i = \Gamma_{i,i}$ if $\Gamma_{i,i} > \sum_{j \neq i} \Gamma_{i,j}$, otherwise, we pick $a_i = 1.2 * \sum_{j \neq i} \Gamma_{i,j}$, where 1.2 is an arbitrary multiplying factor. We choose a parabolic gain shape for the optical amplifiers $G = -4e16 \times (\lambda - 1555 \times 10^{-9})^2 + 15$ decibels, where λ represents the channel wavelength. The β_i values are chosen by a centralized algorithm to achieve a minimum OSNR target of $23dB$. A centralized approach allows easier verification for the simulations, although the game-theoretic nature of the control algorithm does not require centralized planning.

Table 1: Simulation Parameters

Parameter	Value	Units
Channels	8	
Links	1	
OSNR Target	23	dB
Wavelength Spacing	1	nm
Link Alg. Iteration	100	channel steps
Step Size	5000	
P_0	8.3	dBm
Span Loss, L	10	dB
$n_{0,i}$	0.1	% signal

We simulate time-delay realistically as follows. Light in the fiber optic cable propagates at approximately $200,000km/s$. The round-trip propagation time across one optical span of $100km$ is $1ms$. We assume ten optical spans for a total of $10ms$ delay. In addition, we can assume for the purpose of these simulations that the channel algorithms are updated every $10ms$.

We pick $\mu = 0.25 \times \mu^* = 66.25$ as an initial condition for simulation. For the cases $\rho_i = 0.1$, $\rho_i = 0.54$ and $\rho_i = 0.55$, the calculated time bounds are $\tau < 31.6ms$, $\tau < 5.86ms$ and $\tau < 5.75ms$, respectively. Notice that $\rho_i = 0.54$ calculates a time bound of $5.86ms$, yet the system is still stable for $10ms$. This implies the time bound is conservative. From [14], based on the Lyapunov-Razumikhin approach, we calculated time bounds for $\rho_i = 0.1$, $\rho_i = 0.54$ and $\rho_i = 0.55$ to be $\tau < 25ms$, $\tau < 4.6ms$ and $\tau < 4.5ms$, respectively. We see a clear improvement for the time-bounds herein based on theorem 2 and the bound inequality (24).

We next illustrate the conservative nature in the time-delay bounds that still remains despite the use of the more general Lyapunov-Krasovskii theorem 1. For $\rho_i = 0.1$ for all i and using the same parameters as above, but let the round-trip time-delay for the 10 optical spans equal $30ms$. This time-delay value is close to the theoretical bound computed $\tau < 31.6ms$. Figure 3 depicts this case. Notice that the system is still clearly stable with no visible oscillations that would suggest instability. It is not until a time-delay of approximately $80ms$ that the system is clearly on the verge of instability. Figure 4 depicts this case. Despite an improvement in our time-delay bounds, our stability estimates are still conservative.

7. CONCLUSIONS AND FUTURE WORK

In this paper, we applied Lyapunov-Krasovskii theory to study the stability of an optical link using a primal-dual power control algorithm. We derived time-delay bounds that ensure stability based on network design parameters. In addition, we analyzed the scalar single-source single-link case to simplify and compare our results to those of [14]. The scalar analysis showed no improvement in the time-delay bound, but there was a noticeable improvement in the computed time-delay bounds in the general multi-channel simulations.

Future work involves studying the primal-dual control algorithm with the pricing algorithm located at the links rather than the sources. In addition, we need to expand our analysis to general multi-link networks with unique time-delays for each link.

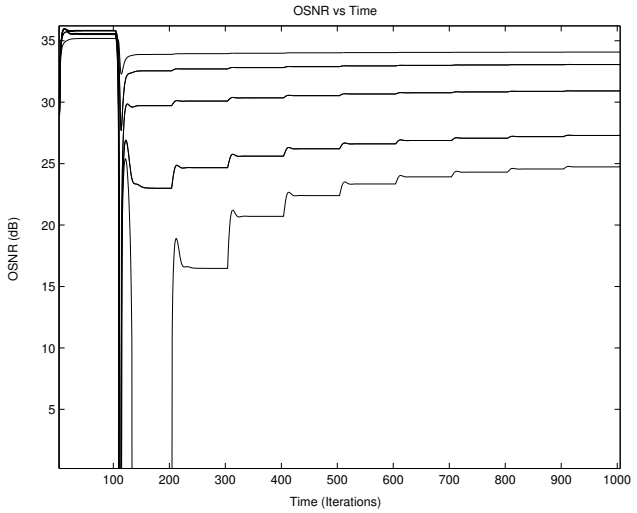

Figure 3: The case $\rho_i = 0.1$ with 10 optical spans and a time-delay of $30ms$

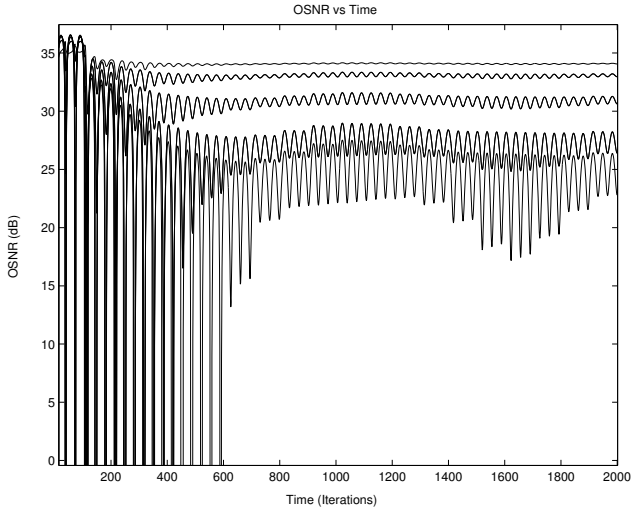

Figure 4: The case $\rho_i = 0.1$ with 10 optical spans and a time-delay of $80ms$

8. ACKNOWLEDGMENTS

The authors gratefully acknowledge the support of the Natural Science and Engineering Research Council of Canada.

9. REFERENCES

[1] O. Ait-Hellal and E. Altman. Stability of abr congestion control using the theory of delayed differential equations. *International Journal of System Science*, 34(10):575–584, 2003.

[2] T. Alpcan and T. Basar. Global stability analysis of an end-to-end congestion control scheme for general topology networks with delay. In *Proc. IEEE Conf. Decision and Control*, pages 1092–1097, December 2003.

[3] J.-M. F. Ana Busic, Tadeusz Czachórski and K. Grochla. Level crossing ordering of markov chains: Computing end to end delays in an all optical network. In *Valuetools 2007: Workshop on Game Theory in Communication Networks*, Nantes, France, October 2007.

[4] K. Gu, V. L. Kharitonov, and J. Chen. *Stability of Time-Delay Systems*. Birkhauser, Boston, 2003.

[5] E. A. Hamidou Tembine and R. El-Azouzi. Asymmetric delay in evolutionary games. In *Valuetools 2007: Workshop on Game Theory in Communication Networks*, Nantes, France, October 2007.

[6] H. K. Khalil. *Nonlinear Systems*. Prentice Hall, New Jersey, 2002.

[7] S. Liu, T. Basar, and R. Srikant. Controlling the internet: A survey and some new results. In *Proc. IEEE Conf. Decision and Control*, pages 3048–3057, December 2003.

[8] F. Mazenc and S.-I. Niculescu. Remarks on the stability of a class of tcp-like congestion control models. In *Proc. 42th IEEE Conf. Decision and Control*, pages 5591 – 5594, Dec. 2003.

[9] F. Paganini, J. C. Doyle, and S. H. Low. Scalable laws for stable network congestion control. In *Proc. IEEE Conf. Decision and Control*, pages 185–190, 2001.

[10] F. Paganini, Z. Wang, J. Doyle, and S. Low. Congestion control for high performance, stability, and fairness in general networks. *IEEE Transactions on Networking*, 13(1):43–55, Feb. 2005.

[11] F. Paganini, Z.Wang, and J.C.Doyle. A new tcp/aqm for stable operation in fast networks. In *2003 IEEE Infocom*, pages 96 – 105, 2003.

[12] L. Pavel. A noncooperative game approach to osnr optimization in optical networks. In *IEEE Conference on Decision and Control*, pages 3033–3038, Dec. 2004.

[13] L. Pavel. An extension of duality to a game-theoretic framework. *Automatica*, 43(2):226–237, Feb. 2007.

[14] N. Stefanovic and L. Pavel. Primal-dual power control of optical networks with time-delay. In *17th IFAC World Congress*, July 2008.

[15] Z. Wang and F. Paganini. Global stability with time delay in network congestion control. In *Proc. IEEE Conf. Decision and Control*, pages 3632–3637, 2002.

[16] Z. Wang and F. Paganini. Global stability with time-delay of a primal-dual congestion control. In *Proc. IEEE Conf. Decision and Control*, pages 3671–3676, 2003.

[17] Z. Wang and F. Paganini. Improved results on global stability of network congestion control based on iterative bounding. In *Proc. IEEE Conf. Decision and Control*, pages 4205–4210, December 2004.

[18] J. Wen and M. Arcak. A unifying passivity framework for network flow control. *IEEE Transactions on Automatic Control*, 49(2):162–174, Feb. 2004.

[19] K. Zhou and J. C. Doyle. *Essentials of Robust Control*. Prentice-Hall, New Jersey, 1998.

APPENDIX

A. LEMMA PROOFS

Proof:[Lemma 2]
We utilize Lyapunov-Krasovskii theory, Theorem 1, to obtain a time-delay bound for the stability of (22). Note that there are more conservative Krasovskii-based theorems [4] that yield both time-independent and time-dependent results, but Theorem 1 is more general and less conservative.

Using Theorem 1, it is shown in [4] by Proposition 5.17, that if we have a system of the form

$$\dot{y} = A_0 y(t) + A_1 y(t-\tau) \tag{59}$$

with a Lyapunov functional (31), then we ensure exponential stability if the following LMI is satisfied

$$\begin{pmatrix} N & PA_1 - Y & -A_0^T Y^T \\ A_1^T P - Y^T & -S & -A_1^T Y^T \\ -YA_0 & -YA_1 & -1/\tau X \end{pmatrix} < 0 \tag{60}$$

where

$$N = PA_0 + A_0 P + S + \tau X + Y + Y^T$$

and $P > 0$ and (32) holds.

From (22), we substitute $A_0 = 0$ into (60) and apply the Schur complement twice to obtain

$$S + \tau X + Y + Y^T < 0 \tag{61}$$

$$\tau A_1^T Y^T X^{-1} Y A_1 - S - (A_1^T P - Y^T)(S + \tau X + Y + Y^T)^{-1}(PA_1 - Y) < 0 \tag{62}$$

In order to simplify our analysis, we select $X = xI$, $Y = \bar{y}I$, and $S = sI$. Then (61) can be rewritten as

$$\tau < \frac{-2\bar{y} - s}{x} \tag{63}$$

From (62), we write the equivalent expression

$$\underline{\sigma}\left(\tau A_1^T Y^T X^{-1} Y A_1 - S - (A_1^T P - Y^T)(S + \tau X + Y + Y^T)^{-1}(PA_1 - Y)\right) > 0$$

where $\underline{\sigma}$ denotes the smallest singular value. Next, we apply Lemma 2.5 from [19], i.e., $\underline{\sigma}(A - B) \geq \underline{\sigma}(A) - \bar{\sigma}(B)$, to get

$$s + \frac{c_1}{s + \tau x + 2\bar{y}} - \frac{\tau}{x} c_3 > 0 \tag{64}$$

where c_1 and c_3 are defined as (25) and (26). Multiply through (64) by $x(s + \tau x + 2\bar{y})$, and group by powers of τ,

$$(-c_3 x)\tau^2 + (x^2 - c_3 s - 2\bar{y}c_3)\tau + (xs^2 + 2\bar{y}xs + c_1 x) < 0 \tag{65}$$

Finally, the bound (24) satisfies (65), and hence (62) is satisfied as well. From (22), we have $A_1 = -\rho\tilde{\Gamma}_a$.

Rewrite (24) as

$$\tau_1 = \frac{j_1 - \sqrt{j_1^2 + j_2}}{2c_3 x} \tag{66}$$

where

$$j_1 = x^2 s - c_3 s - 2\bar{y}c_3 \tag{67}$$

$$j_2 = 4c_3 x^2 (s^2 + 2\bar{y}s + c_1) \tag{68}$$

Note that $x > 0$, $\bar{y} < 0$, and $s > 0$. We make some immediate observations about (66). First of all, a necessary condition is that $\tau_1 > 0$. This is equivalent to

$$j_1^2 + j_2 < j_1^2 \tag{69}$$

where we are assuming, for now, that $j_1 > 0$. This assumption will be proved in the foregoing analysis. From (69), we get

$$j_2 < 0 \tag{70}$$

From (70) and (68), we get the necessary condition

$$s^2 + 2\bar{y}s + c_1 < 0 \tag{71}$$

which also implies that $j_2 < 0$. For (71) to hold, the LHS of (71) must have real roots, or equivalently, $\bar{y} < -\sqrt{c_1}$. Then the bounds on the s variable are

$$-\bar{y} - \sqrt{\bar{y}^2 - c_1} < s < -\bar{y} + \sqrt{\bar{y}^2 - c_1} \tag{72}$$

where we can see the theoretical limits for the bounds in (72) are

$$0 < s < -2\bar{y} \tag{73}$$

when $c_1 = 0$. To prove the previous assumption that $j_1 > 0$, we use (67) to get

$$(x^2 - c_3)s - 2\bar{y}c_3 > 0 \tag{74}$$

where the second term is clearly positive. Thus, if $x^2 - c_3 \geq 0$ then (74) holds and $j_1 > 0$. For $x^2 - c_3 < 0$, then from (74), we get

$$s < \frac{2\bar{y}c_3}{x^2 - c_3} \tag{75}$$

From (73), when $c_1 = 0$ giving (72) its broadest range, then s must satisfy $s < -2\bar{y}$. Thus, to see if the RHS of (75) is ever below the bound $-2\bar{y}$, we impose

$$\frac{2\bar{y}c_3}{x^2 - c_3} < -2\bar{y}$$

which simplifies to

$$-2\bar{y}x^2 < 0$$

which is never true, so the RHS of (75) is always greater than $-2\bar{y}$, and since (72) must hold, then (75) must hold, and $j_1 > 0$.

We can prove that (63) is greater than or equal to (66). To show this, we will attempt to find conditions for when (63) is less than (66), or

$$\frac{-2\bar{y} - s}{x} < \tau_1$$

which simplifies to

$$c_1 < 0$$

which is not possible. By contradiction, (63) is greater than or equal to (66) and hence, we only need on focus on optimizing (66).

End of Proof

Proof:[Lemma 3]

To show exponential stability for the reduced system (21), we take the first derivative with respect to x

$$\left.\frac{df(x)}{dx}\right|_{x=0} = \left.\frac{-\eta 1_{row}\tilde{\Gamma}_a^{-1}\beta}{(x(t)+\mu^*)^2}\right|_{x=0} = \frac{-\eta 1_{row}\tilde{\Gamma}_a^{-1}\beta}{(\mu^*)^2} < 0 \quad (76)$$

where we impose $1_{row}\tilde{\Gamma}_a^{-1}\beta > 0$. Note that $1_{row}\tilde{\Gamma}_a^{-1}\beta = 1_{row}\tilde{\Gamma}_a^{-1}diag(\beta_i)1_{col}$, and for a real matrix A, $v^TAv > 0$ for all v if and only if $v^TA^{-1}v > 0$ for all v. Thus, if (27) holds then $v^T\frac{(\tilde{\Gamma}_a+\tilde{\Gamma}_a^T)}{2}v = v^T\tilde{\Gamma}_a v > 0$, or $\tilde{\Gamma}_a > 0$. This implies that $\tilde{\Gamma}_a^{-1} > 0$, and $\tilde{\Gamma}_a^{-1}diag(\beta_i) > 0$. Hence $1_{row}\tilde{\Gamma}_a^{-1}\beta > 0$. By Corollary 4.3 in [6], the origin of (21) is exponentially stable.

End of Proof